METHODOLOGY   **Open Access**

CrossMark

Hydromechanical constraints on piping failure of landslide dams: an experimental investigation

Austin Chukwueloka-Udechukwu Okeke[*] and Fawu Wang

Abstract

Background: Understanding the internal structure and material properties of landslide dams is essential for evaluating their potential failure mechanisms, especially by seepage and piping. Recent research has shown that the behaviour of landslide dams depends on the internal composition of the impoundment. We here present an experimental investigation of the hydromechanical constraints of landslide dam failure by piping. Experiments were conducted in a 2 m × 0.45 × 0.45 m flume, with a flume bed slope of 5°. Uniform dams of height 0.25 m were built with either mixed or homogeneous silica sands. Uniform-sized pebbles encased in a plastic mesh were used to initiate internal erosion. Two laser displacement sensors were used to monitor the behaviour of the dams during the internal erosion process while a linear displacement transducer and a water-level probe were deployed to monitor the onset of internal erosion and the hydrological trend of the upstream lake.

Results: Five major phases of the breach evolution process were observed: pipe evolution, pipe enlargement, crest settlement, hydraulic fracturing and progressive sloughing. Two major failure modes were observed: seepage and piping-induced collapse. Majority of the dams composed of homogeneous material failed by seepage and downstream slope saturation, whereas dams built with mixed material failed by piping.

Conclusions: We found that an increase in soil density and homogeneity of the dam materials reduced the potential to form a continuous piping hole through the dams. Furthermore, the potential for piping and progression of the piping hole through the dams increased with an increase in the percentage of fines and a decrease in hydraulic conductivity. The rate of pipe enlargement is related to the erodibility of the soil, which itself is inversely proportional to the soil density. This study provides new insights into the governing conditions and breach evolution mechanisms of landslide dams, as triggered by seepage and piping.

Keywords: Landslide dam, Internal erosion, Piping, Hydraulic fracturing, Crest settlement, Breach evolution

Background

Piping is an important hydrogeomorphic process which plays a vital role in the modification of the natural environment. Its widespread occurrence in all climates and in a wide range of soil types may be due to variations in the physicochemical conditions of the environment. Many geomorphological and hydrological studies have been made of the phenomenon of piping, due to its significant contributions to hillslope erosion processes such as gullying and landslides, as well as in the transport of solutes from regions of higher hydraulic head to regions of lower hydraulic head (Masannat 1980; Jones 1994, 2004; Faulkner 2006; Wilson 2011). Nevertheless, piping remains one of the major causes of failure of embankment dams. For example, the 1976 failure of the Teton Dam in Idaho (USA) was triggered by uncontrolled piping on June 3 during the initial filling of the reservoir. The dam failed two days later, claiming 11 lives, with an estimated total damage of about 1 billion dollars. Stene (1995) reported that over 300 million dollars was paid in claims for damage caused by the disaster. Similarly, piping is one of the common failure modes of landslide dams, although the phenomena is rarely observed, due to challenges posed by rugged terrain, which sometimes

* Correspondence: elo_destiny@yahoo.com
Department of Geoscience, Graduate School of Science and Engineering,
Shimane University, 1060 Nishikawatsu-cho, Matsue, Shimane 690-8504,
Japan

limits access to downstream areas. Several examples of the piping failure of landslide dams have been reported in the literature (Glazyrin and Reyzvikh 1968; Costa and Schuster 1988). The 1835 rock and debris avalanche dam that formed Lake Yashinkul on the Tegermach River in the present Republic of Kyrgyzstan is one historic example. This dam failed by piping in 1966, after a lifespan of 131 years (Pushkarenko and Nikitin 1988).

The internal structure of landslide dams plays a vital role in understanding the failure mechanisms of valley-confined deposits, and most importantly, for evaluating the mechanical resistance of landslide dams to failure by either piping or overtopping (Wassmer et al. 2004). Acquiring grain size data is critical for accurate assessment of landslide dams, but limited sedimentological data is available, due to crude sampling methods and the challenges posed by rugged terrain and poorly exposed deposits. Nevertheless, the study of sedimentological characteristics of natural river blockages is imperative for natural hazard assessment studies, as they have a major influence on the overall strength of dams, and control the rate of breach development (Fread 1988; Casagli et al. 2003). Grain size distribution analysis has been used to study the internal structure of some landslide dams (Crosta et al. 2006; Dunning 2006; Duman 2009; Dunning and Armitage 2011; Shugar and Clague 2011; Wang et al. 2013). Field and laboratory analysis of textural characteristics of several landslide dam materials show that they are mostly poorly to very poorly sorted, matrix- or clast-supported, finely skewed, brecciated, stratified to massive sediments, are usually armored with angular boulders, and are sutured with a matrix of very fine materials (Weidinger 2006; Capra 2007, 2011).

Numerous experimental methods have been used to simulate the development of internal erosion and piping in earth dams and landslide dams (Wit et al. 1981; Brauns 1985; Maknoon and Mahdi 2010). Hanson et al. (2010) analyzed variation in erodibility of different soil materials due to internal erosion in dams by conducting large-scale outdoor model tests. They observed that the rate of erosion in differing soil materials varied in orders of magnitude. Marot et al. (2012) used a triaxial cell device coupled with a hydraulic system to study the influence of angularity of coarse fraction grains on the internal erosion process. They concluded that the angularity of coarse fraction grains may increase the erosion resistance of the tested soils by a factor of five. Richards and Reddy (2012) performed laboratory experiments on the initiation of backward erosion in cohesive and non-cohesive soils using a triaxial test device called a true triaxial test apparatus. They observed that the primary mode of failure of non-cohesive soils was by backward erosion, which required a seepage velocity of $0.8 \sim 1.1$ cm/s to initiate piping in uniformly graded sands.

Ke and Takahashi (2012) studied the mechanical effect of internal erosion on gap-graded non-cohesive soils by conducting one-dimensional seepage tests using a fixed-wall permeameter. These authors concluded that the onset of internal erosion is indicated by loss of fine material, coupled with a significant increase in hydraulic conductivity.

Significant results have been obtained from experimental studies using triaxial cell chambers, constant-head permeameter, and other laboratory methods such as hole erosion tests (HET) and jet erosion tests (JET). However, none of these methods have simulated the potential failure mechanisms of landslide dams triggered by internal erosion and piping. This paper presents a series of experiments conducted to investigate the hydromechanical constraints of soils on the development of internal erosion and piping in landslide dams. The experiments were performed in a flume equipped with monitoring sensors and transducers capable of recording transient changes during the process. The two main objectives of this research are: (1) to identify the various failure mechanisms of landslide dams under varying hydromechanical properties of the materials forming the dams, and (2) to evaluate and infer the probable physical properties of dam materials and conditions most appropriate for long term stability of such dams. The research methodology aims at providing new ideas and insights on stability analysis of landslide dams, considering the sparse research to date on the material properties of landslide dams which are relevant in dam breach analysis and flood routing.

Experimental methods

Trapezoidal-shaped landslide dams were built in the laboratory after a series of field investigations were carried out on two recent landslide dams (Akatani and Kuridaira landslide dams) formed in 2011, in the Kii Peninsula of southwest Japan. The choice of these sites as reference cases for this study was prompted by several factors, including (1) the relatively large volume of the two impoundment materials, of 9.4 million m³ and 13.9 million m³, respectively, (2) the characteristic nature of the landslide dam materials, which are dominantly composed of disjointed angular boulders (averaging $1 \sim 10$ m in diameter), and cobble-sized clasts sutured in a fine-grained matrix (Fig. 1a), and (3) the significance of drainage pipes buried in the two sites, which function as artificial drainage channels for lowering of the upstream lake, so as to avoid potential overflow (Fig. 1b). The experimental dams were built to partially reproduce the geometry of landslide dams in real case scenarios, with efforts made to minimize unavoidable scaling issues resulting from space and time constraints.

Fig. 1 a Exposed section of the materials composing the Akatani landslide dam **b** Upstream side of the Akatani landslide dam showing water inflow into the dam through an artificial drainage pipe. Note: People for scale (photo by Wang FW)

Experimental setup

The experiments were carried out in a rectangular flume tank specifically designed for this study. Prior to the construction of the tank, the size, scale, and position of the dam model were considered to enable timely collection of accurate data. The flume tank was 2 m long, 0.45 m high and 0.45 m wide, and was made entirely of glass, with two 4 cm diameter drainage outlets at the downstream end to allow steady discharge of fluidized sediments. The flume was gently tilted to make a bed slope of 5°. The construction and modification of the flume tank considered the dimensions of other flume tanks used by previous studies, including the 1 m × 0.6 m × 0.45 m model used by Sidle et al. (1995), 5 m ×

0.3 m × 0.5 m (Awal et al. 2009), 1.5 m × 1 m (Wilson 2009), 1.4 m × 1 m (Wilson 2011), and 0.5 m × 0.5 m × 0.5 m (Fox et al. 2014) flumes. The upstream lake was recharged from a drainage hose fed by a water tap. Pre-failure crest settlements associated with the onset of internal erosion and piping were measured with two CMOS multi-function analog laser displacement sensors attached to a wooden overboard. Concave-upward depressions observed during the initiation of internal erosion and piping were monitored by positioning one of the sensors (H_{d1}) directly above the center of the dam crest, while the other sensor (H_{d2}) was fixed 0.07 m from the central part of the crest. These measurements were made by allowing a maximum vertical distance of
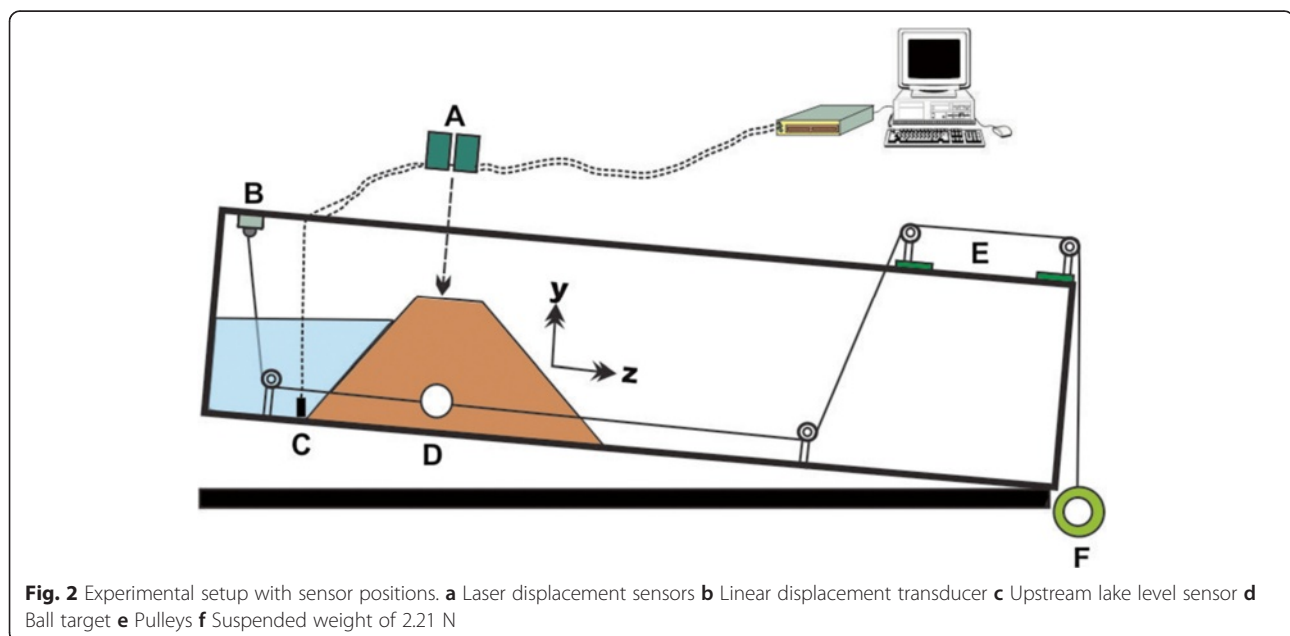
0.25 m between the dam crest and the sensor heads. Lateral displacements and downstream transport of eroded soil particles were measured using a linear displacement transducer (LDT) with a maximum response speed of 0.2 m/s and a measuring range of 1.0 m. The transducer was fixed at the upper end of the flume tank, and a thin metallic wire attached to the sensor head was connected to a plastic ball of similar weight to the materials used in the experiments. The ball was buried at the center of the dam crest, while the outer end of the metallic wire, suspended by a known weight, passed through four stationary pulleys. Transient changes in the upstream water levels were tracked with a pore-water pressure sensor with a rated capacity of 50 kPa. The pore-water pressure sensor was fixed at a stationary position near the upstream dam toe to ensure accurate measurement and recording of data. All these sensors were connected to a standard real-time monitoring and recording unit comprised of a universal recorder (KYOWA EDX-100A) and a computer. The experimental setup was designed to simulate (1) the internal erosion process and piping development in relation to the nature of the material forming the impoundment; (2) the failure mechanisms of landslide dams made of materials of varying geotechnical properties; and (3) the rate of development of piping. Two digital video cameras were strategically positioned to record the failure sequence of the dams.

Experimental procedure and properties of the soils used

A schematic diagram of the experimental setup with the location of sensors and workstation used in the recording of data is shown in Fig. 2. The dam models were built 0.4 m downslope from the upstream water inlet

and were uniformly compacted by gently tapping successive five cm thick soils laid on the floor of the flume tank, using a wooden mallet. Friction was increased at the sides of the flume by ensuring maximum compaction of soil near the flume wall. Internal erosion was initiated by laying uniformly sized pebbles encased in a plastic mesh at the center of the dam. The encased pebbles were laid such that a flume bed slope of 10° was obtained (Fig. 3). The plastic ball attached to the linear displacement transducer was laid in the dam and held at critical tension by a suspended weight. The dam models were built at constant upstream and downstream slope angles of 35° and 50°, respectively. Prior to the start of each experiment, the pore-water pressure sensor was immersed in a water-filled jar for several minutes to ensure accurate measurement. A manually-operated flow meter with an initial discharge set at 1.2×10^{-4} m^3/s was used to control the rate of inflow into the upstream lake. The flow rate was maintained until the upstream water level reached two-thirds of the dam height, at which stage water began to flow into the dam through the artificial channel. This filling strategy was adopted because the overtopping failure of landslide dams was not considered in this study.

The stability of landslide dams is, to a certain degree, controlled by the nature of the materials composing the dams. Landslide dams are generally composed of fragmented materials which have a wide range of sediment sizes (Costa and Schuster 1988; Schuster 1995; Davies and McSaveney 2011; Dunning and Armitage 2011). Reproducing field prototypes of landslide dams in a flume is challenging, especially with respect to downsizing the impoundment materials to laboratory-scale experiments.
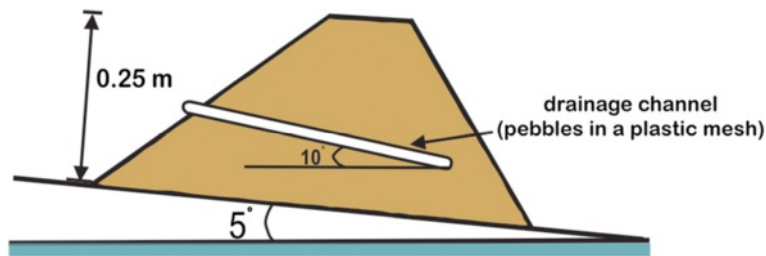

Fig. 2 Experimental setup with sensor positions. **a** Laser displacement sensors **b** Linear displacement transducer **c** Upstream lake level sensor **d** Ball target **e** Pulleys **f** Suspended weight of 2.21 N

Fig. 3 Schematic diagram of the landslide dam geometry

Consequently, the materials used in this study comprised mixed and homogeneous samples of industrial silica sands (numbers 4, 5, 6, 7, and 8) in varying proportions (Figs. 4 and 5). The mechanical and hydraulic properties of the dam materials are given in Table 1. In the first step of the experiments, 2000 ml of water and 40 kg of each material were rigorously mixed using a mechanical mixer. The soil samples were used to build dams of a uniform crest and height (H_d) of 0.1 m and 0.25 m, respectively (Fig. 6). Summaries of the characteristics of the experiments carried out on dams built with mixed and homogeneous materials are given in Tables 2 and 3, respectively. The initial discharge rate Q_i was constant in all experimental runs, whereas T_e and T_b represent the time of onset of internal erosion and time of dam crest collapse, respectively.

Results and discussion
Observed phases of the breach evolution process
Several phases of the breach evolution process were observed during repeated experiments. Qualitative assessments and observations, coupled with data obtained from precision sensors, helped to distinguish the various stages. The breach development processes observed included (1) pipe development, (3) pipe enlargement, (4) crest settlement, (4) hydraulic fracturing, and (5) progressive sloughing. While the breach development process followed the sequence listed above in some dams, others failed retrogressively, resulting in late-stage overtopping of the dams. Therefore, before describing the results, it is pertinent to define and describe the various failure phases observed in this study.

Pipe development
This process is related to the formation of a continuous piping hole, as a result of increased action of seepage forces through the soil micropores. The initial stage of this process starts with the initiation of internal erosion, which in this case, was enhanced by concentrated seepage through the artificial drainage channel. An abrupt drop in velocity of the seeping water at the opposite end of the drainage channel, about 5 cm before the downstream slope face, reduces the pressure of the seeping water through the soil micropores. However, the erosive
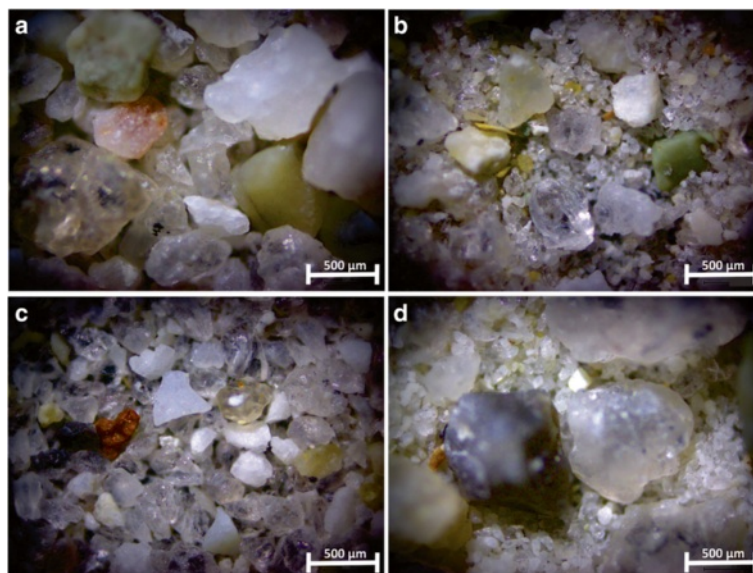

Fig. 4 Photomicrographs of reconstituted materials of dam mixes (**a**, **b**, **c** and **d**) (photo by Okeke AC)

Fig. 5 Photomicrographs of homogeneous materials of dam mixes (**e**, **f**, **g** and **h**) (photo by Okeke AC)

cycle continues as a result of high pore-water pressure, leading to a partial reduction of the shear strength of the soil, as observed at the downstream slope face in the form of a '*wet spot*'. Summarily, the numerous complex mechanisms leading to the initiation of internal erosion and subsequent development of a piping hole include (1) generation of high pore-water pressure due to the incessant action of the seepage flux, which reduces the apparent cohesion of the soil, (2) increase in seepage forces through the soil micropores, which reduces the effective stress of the soil and produces drag forces sufficient for soil particles to be detached and entrained downstream, and (3) gradual evolution of the existing micropores, essentially caused by the hydraulic shear stress exerted by the seeping water. A continuous pipe is formed through the dam once appreciable aggregates of soil particles are removed and transported downstream by the flowing water. From observation during the experiments, it was noted that at the onset of the pipe development process,

the initial diameters of the developing pipes were mostly smaller than or equal to the diameter of the artificial drainage channel.

Pipe enlargement
The mechanism of pipe enlargement can be related to the effect of the hydrodynamic forces produced by the flowing water on the hydromechanical properties of the soil under varying physicochemical conditions. The evolution of the pipe through the dam changes the dynamics of the seeping water from low-pressure flow through the soil micropores to high-pressure flow through the enlarging pipe. At this stage, the enlargement of the pipe and subsequent progression of the breaching process is usually rapid, and thus depends on several properties of the soil, including the interlocking effect, the shear strength, and density of the soil, as well as the energy of the flowing water. The tractive force theory based on the bed load formula suggests that the amount of sediment

Table 1 Mechanical and hydraulic properties of the dam materials D_{50} is mean grain size, C_u is coefficient of uniformity, C_c is coefficient of curvature, ρ_{dry} is dry bulk density, e_o is the initial void ratio, n is porosity, and k is coefficient of permeability

| Sample name	D_{50} (mm)	C_u (mm)	C_c (mm)	ρ_{dry} (Mg/m³)	e_o	n (%)	k (m/s)
Dam mix A	0.236	4.051	0.993	1.33	0.99	49.7	3.9×10^{-6}
Dam mix B	0.358	5.887	2.407	1.30	1.04	51.0	3.1×10^{-4}
Dam mix C	0.186	3.393	0.883	1.19	1.23	55.2	4.8×10^{-5}
Dam mix D	0.118	1.990	0.852	1.22	1.17	53.9	1.1×10^{-5}
Dam mix E	0.799	2.474	1.385	1.21	1.19	54.3	3.2×10^{-4}
Dam mix F	0.235	1.310	0.990	1.18	1.25	55.6	6.1×10^{-4}
Dam mix G	0.264	2.315	0.947	1.15	1.30	56.5	8.2×10^{-4}
Dam mix H	0.124	1.726	1.195	1.02	1.59	61.4	5.8×10^{-5}
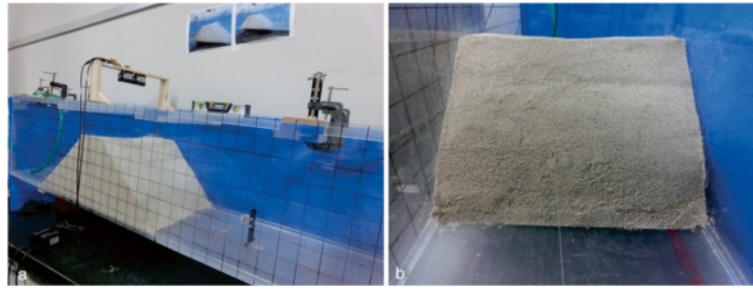
Fig. 6 a Side view of the flume tank. **b** Front view of a dam showing the downstream slope prior to commencement of an experiment (photo by Okeke AC)

transported per second per unit width of a conduit q_s is a function of shear stress τ (Singh 1996):

$$q_s = f(\tau) \tag{1}$$

Thus, the erodibility of the soil at the periphery of the flow path and the hydraulic shear stress are two key factors which determine the rate of erosion and the time of progression through to completion of the breaching process. The complexity of the pipe enlargement process with respect to sediment transport mechanics has been described by the excess shear stress equation:

$$\varepsilon = k_d(\tau_a - \tau_c)^a \tag{2}$$

where ε is the sediment transport rate (m/s), k_d is the erodibility coefficient (m³/N-s), τ_a is the hydraulic shear stress on the soil boundary (Pa), τ_c is the critical shear stress (Pa), and a is an exponent, usually assumed to be 1 (Hanson and Cook 1997; Fell et al. 2003). Enlargement of the pipe depends on the ability of the material to support the pipe roof. Hence, observations from the series of experiments showed that most of the homogeneous dams failed by progressive saturation of the downstream slope. In contrast, well-defined piping holes were formed in dams composed of mixed materials with a higher piping tendency, as evident in dam mixes *D* and *H,* where the pipe roofs survived for a relatively longer time.

Crest settlement

This phenomenon was observed in all the experiments, but the evolution process varied with the material forming the dam. In this case, crest settlement is related to the formation of a concave-upward depression at the center of the dam crest, as a result of internal erosion and piping within the material underlying the dam crest. This phenomenon is usually initiated by seepage forces through the dam, and can be associated with several other processes, such as soil arching, cracking, and hydraulic fracturing. The effect is more pronounced in low-density fine-grained soils and cohesionless soils with high void ratios, in which the development of very high pore-water pressure conditions leads to the reduction of the effective stress of the soil. Crest settlement was more evident in dams built with homogeneous materials than in those built with reconstituted materials, excluding dams containing a significant amount of fines, such as dam mixes *D* and *H*.

Hydraulic fracturing

This failure mechanism is common in dams built with reconstituted materials. The hydraulic fracturing process is initiated by differential settlement, arising from the different compressibilities of the soils, coupled with uneven compaction. This leads to the development of tensile stresses in weak or soft zones as pore-water pressure increases through the dam. Observations during the experiments found that as soon as the upstream lake level reached the tip of the encased pebbles, seepage forces converged into the pebbles and any other hydraulically weak zone, leading to erosion of soil particles along the developing conduit. The crack formation can be related to increased pore-water pressure, which reduces the minor effective principal stress across the plane of the crack ($\sigma_3 < 0$). This further implies that hydraulic fractures occur once the pore-water pressure in the dam is

Table 2 Summary of experiment carried out for dams composed of mixed materials

Run series	Material	Composition (%)	T_e (s)	T_b (s)	Characteristic features
1	Dam mix A	Equal amounts of SS 4, 5, 6, 7 and 8	90	160	Piping and hydraulic fracturing
2	Dam mix B	SS-5 and SS-8 (70:30)	98	145	Piping followed by pipe roof collapse
3	Dam mix C	SS-6 and SS-8 (30:70)	82	158	Piping followed by pipe roof collapse
4	Dam mix D	SS-4 and SS-8 (30:70)	86	184	Well-defined piping hole which supported the pipe roof

Table 3 Summary of experiments carried out for dams composed of homogeneous materials

Run series	Material	Composition (%)	T_e (s)	T_b (s)	Characteristic features
1A	Dam mix E	SS-4 (100)	80	240	Seepage;
					Downstream slope saturation;
					Toe bulging followed by slope unraveling
2A	Dam mix F	SS-5 (100)	85	195	Seepage;
					Downstream slope saturation;
					Toe bulging;
					Progressive sloughing
3A	Dam mix G	SS-6 (100)	75	230	Poorly developed piping hole;
					Downstream slope unravelling
4A	Dam mix H	SS-8 (100)	60	260	Formed well-defined piping role;
					Supported the pipe roof

greater than or equal to the total stress σ_3, or equal to the tensile strength of the soil, σ_t (Mattsson et al. 2008).

Progressive sloughing

This type of failure was observed in dams built with very loose cohesionless materials (dam mixes *E*, *F*, and *G*), and to a lesser extent in dams built with dam mixes *A* and *B*, but was rarely seen in dams built with very fine sand and silt. The process is often triggered when the seepage forces are less than or equal to the shear strength of the soil. Thus, the inability of the seeping water to produce sufficient drag forces needed to dislodge and entrain the soil particles and form a continuous piping channel leads to gradual seepage flow towards the downstream slope. The saturation of the downstream slope due to seepage leads to the reduction of the effective stress of the soil and subsequently causes very small slumps and slides in the form of cantilever failures to occur at the toe of the slope. This, in turn, leaves very steep faces which fail under increased pore-water pressure. This cycle of failure continues until the exposed section of the dam yields to the effect of increased pore-water pressure, and slides downstream, leading to the partial breaching of the dam.

General description of the experiments

The initial condition set for the experiments assumed that either the dammed lake is of low discharge or the location where the landslide blocked the valley is relatively 'dry' (Korup 2004). Hence, no tailwater was present at the downstream area, since the slope of the flume tank was 5°. After building the dam model, the upstream lake level was gradually increased until the water reached the tip of the encased pebbles. The hydrological trend and failure mechanisms of the dams were largely controlled by the hydromechanical properties of the soil materials. The two major failure modes observed were seepage and piping. While piping failure was

dominant in dams composed of very fine materials or mixed soils with an appreciable amount of fines, seepage, and downstream slope saturation were dominant in dams built with homogeneous cohesionless soils.
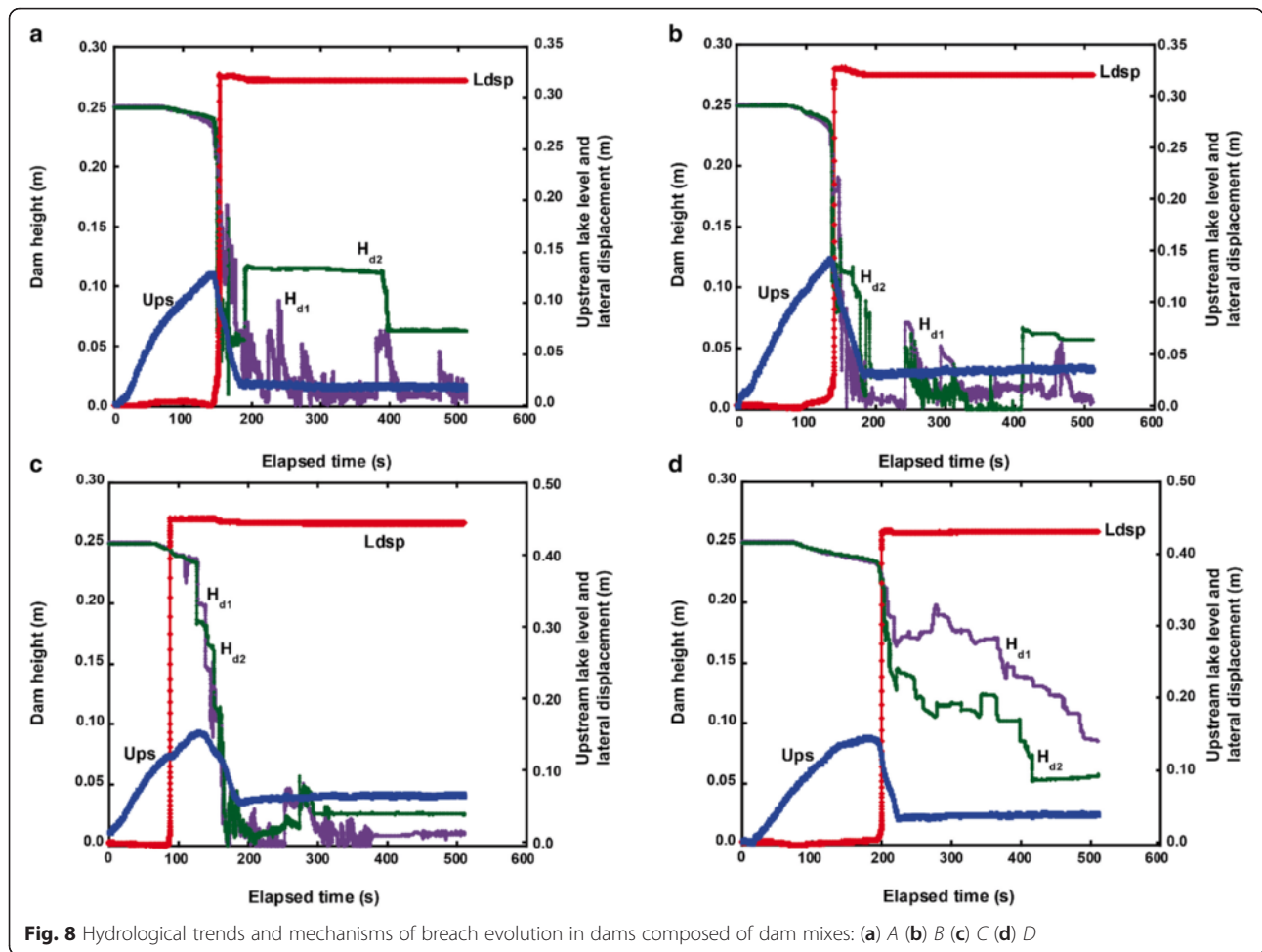
The first physical defects observed during the experiments were the formation of longitudinal cracks at the upper part of the upstream slope, as the level of the upstream lake rose with time. This was usually followed by the settlement of the entire dam, and subsequent formation of concave-upward depressions at the center of the dam crest. The rapid increase in seepage gradient along the encased pebbles enhanced initiation of internal erosion at the boundary between the dam material and the encased pebbles. Progression of internal erosion through the dam was manifested by the appearance of a *wet spot* on the downstream slope (Fig. 7a). Generally, two primary transverse cracks are formed near the left and right banks of the dam. With time, these transverse cracks were crosscut by miniature cracks from which small slumps and slides may occur. Evolution of the piping hole at the downstream slope could be rapid or may collapse instantaneously, depending on the shear strength of the dam material (Fig. 7b). The breaching process continued with enlargement of the piping hole due to steady saturation, and subsequent collapse of the pipe wall through existing cracks and weak zones on the slope (Fig. 7c). The piping hole diameter increased with corresponding increase in the discharge through the dam, causing a rapid drawdown of the upstream lake. The pipe roof collapsed once pore-water pressure was greater than or equal to the effective stress of the dam material (Fig. 7d). The collapse of the pipe roof led to a gradual rise in the upstream lake until the energy of the eroding medium was able to dislodge and transport the collapsed sediments downstream. The experiments ended by the formation of a wide breach channel, with base width ranging from 0.1 m to 0.35 m (Fig. 7e).

Fig. 7 Evolution of the breaching process **a** Wet spot at the downstream slope **b** Formation and growth of a piping hole **c** Pipe progression and enlargement **d** Pipe roof collapse **e** Final breach profile of the dam (Okeke et al. 2013)
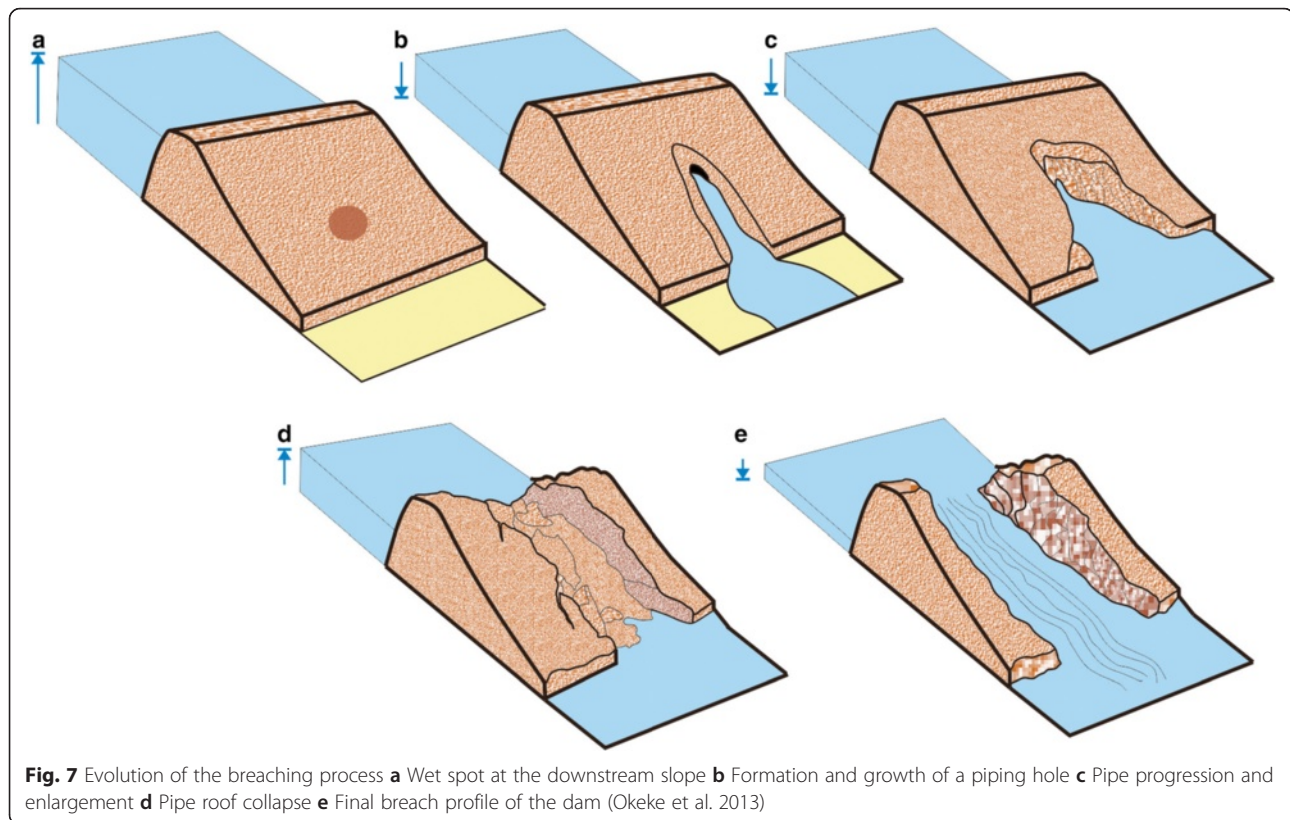
Failure mechanisms of dams built with mixed materials

Four representative experiments were carried out to assess the potential for piping and failure of dams composed of mixed materials of varying physical properties (Table 2). The characteristic physical properties of the reconstituted materials influenced the stage hydrographs and the deformation behaviour of the dams. The potential for formation of a continuous piping hole through the dams increased with an increase in percentage fines content. The mechanism of failure of the dams was primarily initiated by piping, although the likelihood of the developing pipe to form a uniform cylindrical hole varied with the density and magnitude of shear stress exerted by the seeping water. Similarly, the ability of the dam material to support the roof of the piping hole varied with the amount of fines in the soil. Visual observations show that the dam mix *D* material (Run series 4) manifested higher tendency of sustaining the roof of the piping hole in comparison with other materials, where the roof of the poorly developed piping holes collapsed under steady propagation of the wetting front. Hydraulic fractures caused by internal stress redistribution increased with an increase in heterogeneity of the materials. Figure 8 shows the hydrological trends and mechanisms of breach evolution in dams composed of mixed materials. A steady rise in upstream lake level

initiated a hydraulic head gradient that produced seepage forces through the dams. This consequently led to the formation of concave-upward depressions, mostly at the center of the dam crest. The formation of these depressions on the dams may be attributed to internal instability caused by suffusion which triggered the development of extensive cracks and soft zones (Fig. 9). The rate of change of volume (settlement) of the unsaturated dam materials and the decrease in shear strength may be attributed to the relationship between wetting front propagation and the hydromechanical properties of the materials. The onset of internal erosion is marked by buckling of the ball target due to loss of tension induced by the shear stress of the seeping water. It is interesting to note that the progression of seepage and formation of a piping hole coincided with lowering of the upstream lake level (as a result of steady discharge through the piping hole), and retraction of the ball target attached to the linear displacement transducer. The results indicate that the progression and enlargement of the piping hole were controlled by cohesion, grain size distribution, particle density and energy of the eroding medium. The general deformation behaviour of the dams composed of heterogeneous and anisotropic cohesionless materials was characterized by the formation of cracks (longitudinal and transverse) aligned perpendicular and parallel

Fig. 8 Hydrological trends and mechanisms of breach evolution in dams composed of dam mixes: (**a**) *A* (**b**) *B* (**c**) *C* (**d**) *D*

to the dam axis. The final stage of the breach evolution process was marked by formation of a wide breach channel with base width ranging from 0.1 m to 0.25 m.

Failure mechanisms of dams built with homogeneous materials

The failure mechanisms of dams composed of homogeneous and isotropic cohesionless materials were assessed with four different soils (Table 3). A steady rise in upstream lake initiated a hydraulic head which enhanced concentrated seepage through the artificial drainage channel. Propagation of wetting front was observed to occur at rates higher than those observed in dams built with mixed materials. Steady propagation of wetting front within the unsaturated cohesionless dam materials resulted in a decrease in matric suction (negative pore-water pressure) which caused a reduction in interstitial voids, as evidenced by the formation of concave upward depressions at the central part of the dam crest. Figure 10 shows the hydrological trends and failure mechanisms of dams built with homogeneous and isotropic cohesionless materials. The onset of internal erosion and mobilization

of the soil particles adjacent to the drainage channel coincided with buckling of the ball target and formation of cracks, thereby triggering initial deformation of the dam crest. Internal redistribution of stresses initiated by intense seepage led to several processes including hydraulic cracking, dam crest settlement, downstream face saturation and toe bulging, and downstream slope unraveling. The majority of these processes were apparent in experiments conducted with dam mixes *E, F,* and *G*, where steady seepage through the dams resulted in exfiltration, sapping erosion, undercutting and sloughing of the partially liquefied soil. In contrast, the experiment conducted with dam mix *H* revealed a well-formed piping hole that lasted for a relatively longer time (Fig. 11). The rapid drawdown of the upstream lake level could be related to the rate of enlargement of the piping hole due to the erosive forces of the seeping water, which continued until the material supporting the pipe roof collapsed into the channel. The results indicate that the potential to form a piping hole through the dams decreased with an increase in density and hydraulic conductivity.
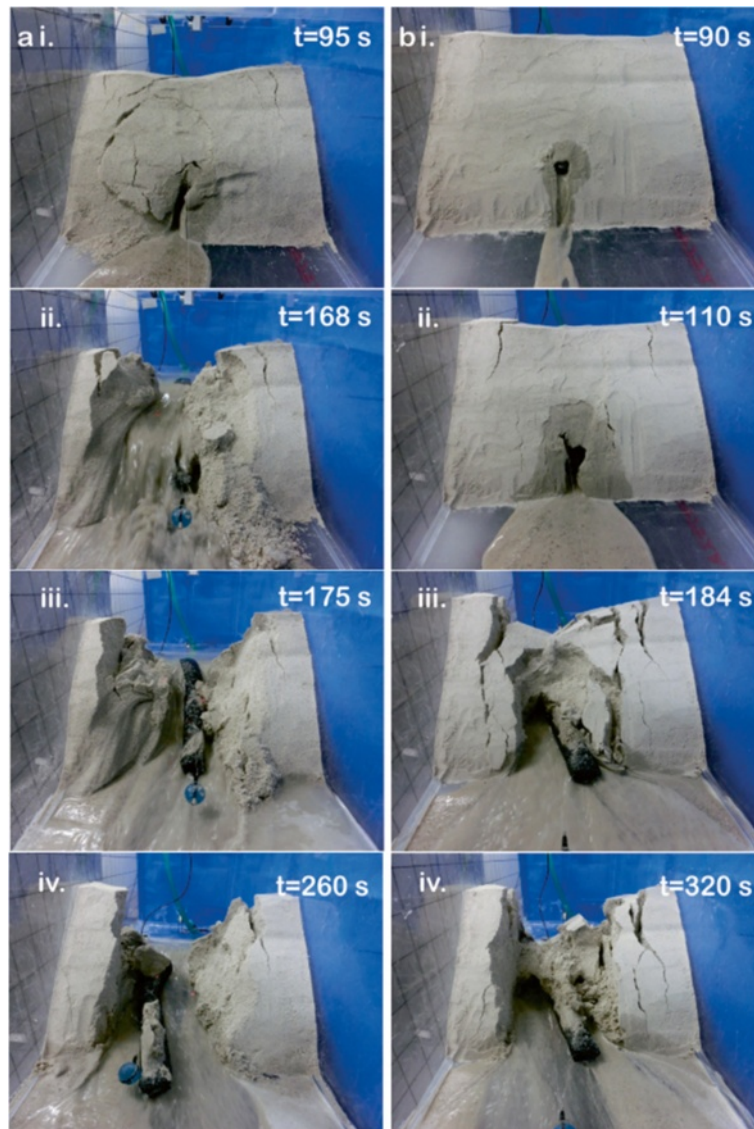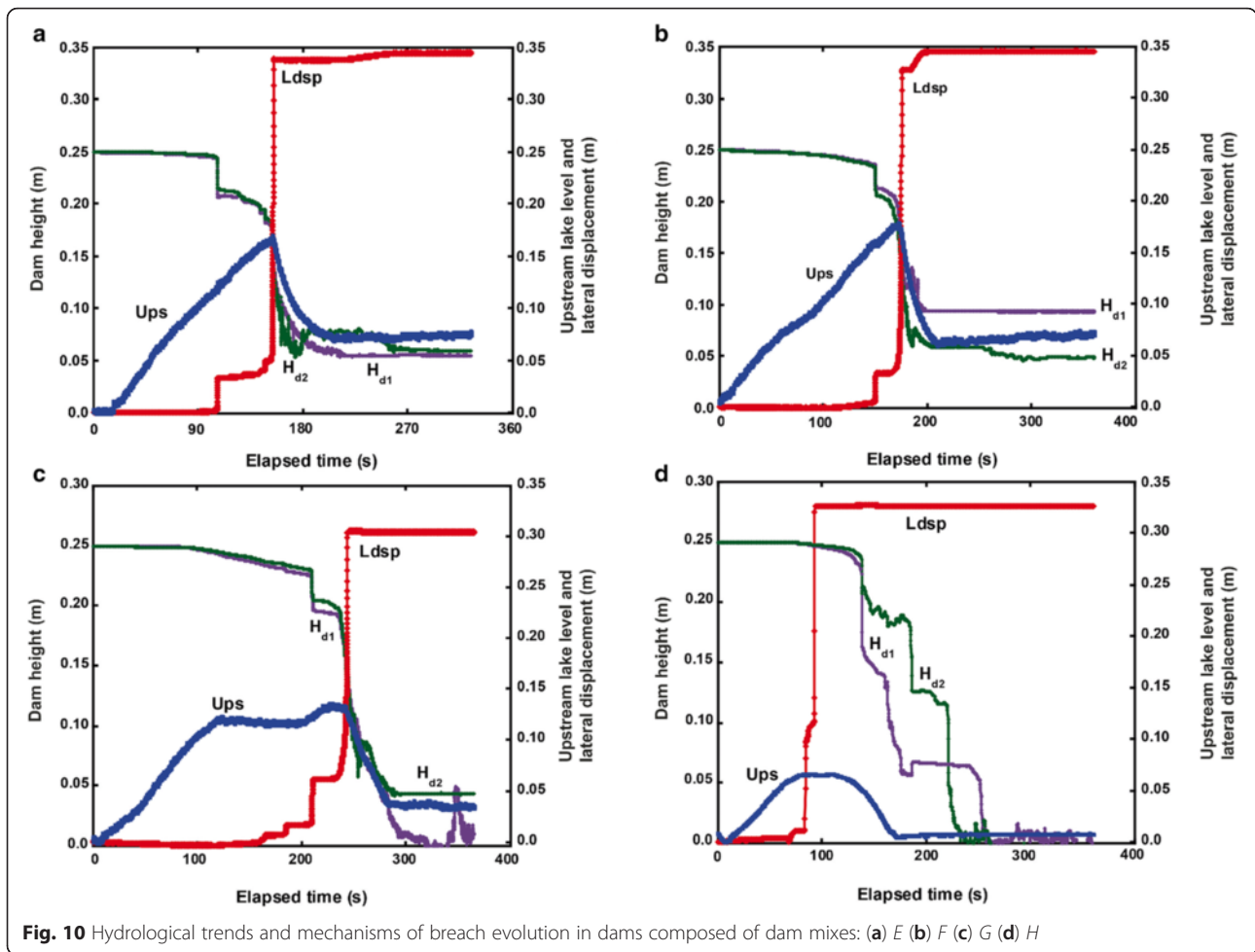
Fig. 9 Failure mechanisms of dams built with **a** dam mix *A* and **b** dam mix *D* showing piping and subsequent collapse of the dam crest (photo by Okeke AC)

Effect of density on erodibility of the dam materials

Figure 12 shows the relationship between the time of collapse of the dam crest, T_b and dry bulk density of the various soils composing the dams. Variations in hydromechanical behaviour were more evident in dams composed of soils of lower density than in those built with soils of higher density. An exception to this case was dam mix D (T_b, 184 s), where the interlocking bonds between very fine particles of silica sand 8 and coarser particles of silica sand 4 at optimum water content seemed to be stronger than in other soil samples. Previous studies of internal erosion and soil erodibility observed that progression of the piping hole and erodibility of material at the periphery of the piping hole depended

on the compaction density and water content (Hanson and Robinson 1993; Fell et al. 2003). Field erodibility tests conducted by Chang et al. (2011) on two landslide dams triggered by the 12 May 2008 Ms 8.0 Wenchuan earthquake in Sichuan Province of China showed that an increase in bulk density was inversely proportional to the coefficient of erodibility with depth. Furthermore, large-scale physical tests carried out by Hanson et al. (2010) in their investigation of the impact of erosion resistance on internal erosion in embankment dams identified that erosion resistance for the same embankment material increased with an increase in compactive effort and water content. Observations made during the experiments in our present study yield similar results.

Fig. 10 Hydrological trends and mechanisms of breach evolution in dams composed of dam mixes: (**a**) *E* (**b**) *F* (**c**) *G* (**d**) *H*

Similarly, a comparison between the failure process of run series 4 (dam mix *D*) and run series 2A (dam mix *F*) shows that even at a higher erosion rate q_s, the breach evolution process of the two dams varied greatly. Figure 13 shows the relationship between the initial void ratio of the dam materials and the time of collapse of the dam crest (T_e and T_b). The time of onset of internal erosion, T_e, and the time of dam crest collapse, T_b, reveals the effect of internal instability caused by suffusion. This led to early initiation of internal erosion in dams composed of mixed materials, even at lower void ratios, due to selective removal of fines from the soil matrix and subsequent destabilization of the soil structure. This result indicates that void ratio and other physical properties such as permeability, percentage fines content, and density affect the initiation and progression of internal erosion in dams. Furthermore, the relationship between initial void ratio and the dimensionless settlement index S_I (Fig. 14), clearly shows the behaviour of the dam materials as pore-water pressure and seepage gradient increased through the dams:

$$S_I = \frac{s}{1000 \times H \ \log\left[\frac{t_2}{t_1}\right]} \tag{3}$$

where s is crest settlement in mm between times t_1 and t_2, and H is the dam height in meters (Charles 1986). The general deformation behaviour of the dams shows that settlement increased with an increase in void ratio. Low density cohesionless soils with high void ratios, such as silts, are generally brittle, and thus are prone to cracking during differential settlement. This process is usually associated with the formation of tension cracks and other weak zones of low stress condition. A typical example is the Red Willow Dam in southwest Nebraska, USA. The dam is a 38.4-m high homogeneous embankment made up of low plasticity silts. Emergency investigations conducted by the US Bureau of Reclamation discovered sinkholes at the downstream face, whereas cracks appeared above the outlet works conduit and other locations near the right abutment. The brittle nature of the embankment material coupled with the low
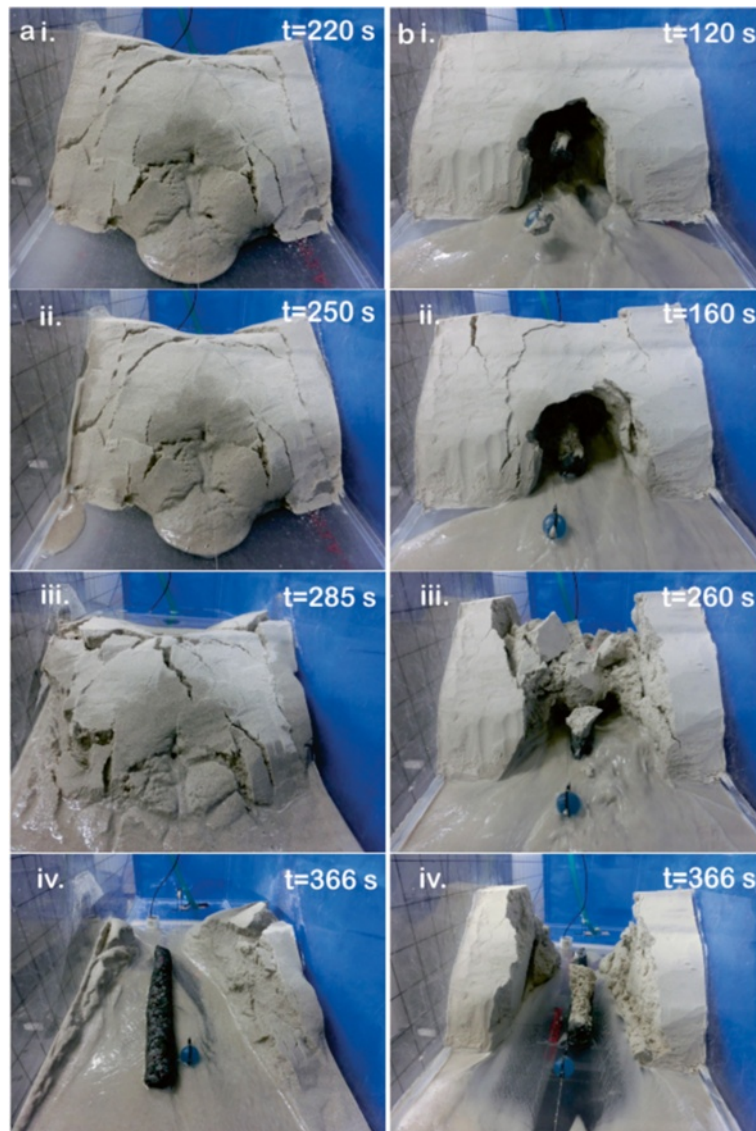
Fig. 11 Failure mechanisms of dams built with **a** dam mix *G* and **b** dam mix *H* showing hydraulic cracking, downstream face saturation and piping (photo by Okeke AC)

density and plasticity index of the soil led to the settlement of the crest to about 1.2 m below the original height, which caused the reservoir level to be lowered.

Natural analogues of seepage and piping in landslide dams
As mentioned before, the potential for seepage and piping failure of landslide dams can be attributed to the textural and sedimentological properties of the impoundment material, as well as the hydrological characteristics of the upstream lake. From a sedimentological perspective, the likelihood of piping and seepage failure of rock avalanche dams is high in comparison with landslide dams that preserved the original stratigraphy of their source rock. A vast number of rock avalanche dams are comprised of

fragmented materials and are mostly characterized by a binary internal structure consisting of: (1) a highly pulverized and matrix-supported basal layer which is very erodible but has low permeability because of its low void ratio, and (2) an upper layer dominated mostly by a coarse blocky carapace of disjointed angular boulders, with large void spaces that support internal erosion (Davies and McSaveney 2011; Strom 2013). Similarly, Dunning et al. (2006) identified three distinct sedimentological facies in rock avalanche dams: the *Carapace*, *Body* and *Basal facies*. The high hydraulic conductivity of the *Carapace facies* and the relative nature of its unstructured comminuted mass serves as a channel for seepage erosion and piping. This phenomenon is analogous to the 1992 failure of the Rio
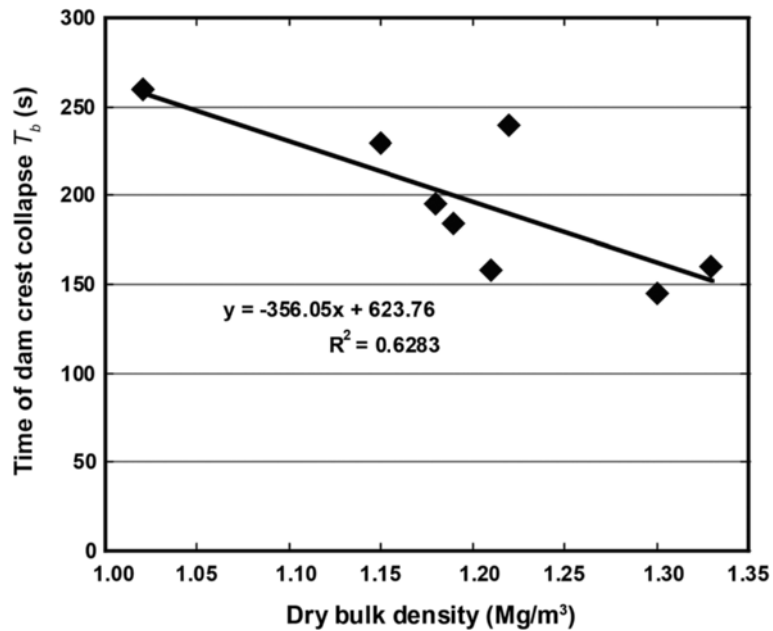
Fig. 12 Relationship between time of dam crest collapse T_b and dry bulk density

Toro landslide dam in Alajuela Province of Costa Rica. The dam failed by seepage and piping when the upstream lake level reached an elevation of 934 ~ 936 m and seeped into the upper pervious and blocky carapace layer, resulting in progressive failure and undermining of the downstream slope (Mora et al. 1993). Another similar event is the 2004 failure of the Tsatichhu landslide dam in Bhutan, which failed by a combination of dam face saturation and progressive seepage through the upper *Carapace facies* (Dunning et al. 2006). The failure mechanisms of these two natural analogues displayed similar characteristics to the results of our present study.

Conclusions

A comprehensive experimental investigation was conducted to study the hydromechanical constraints of soils
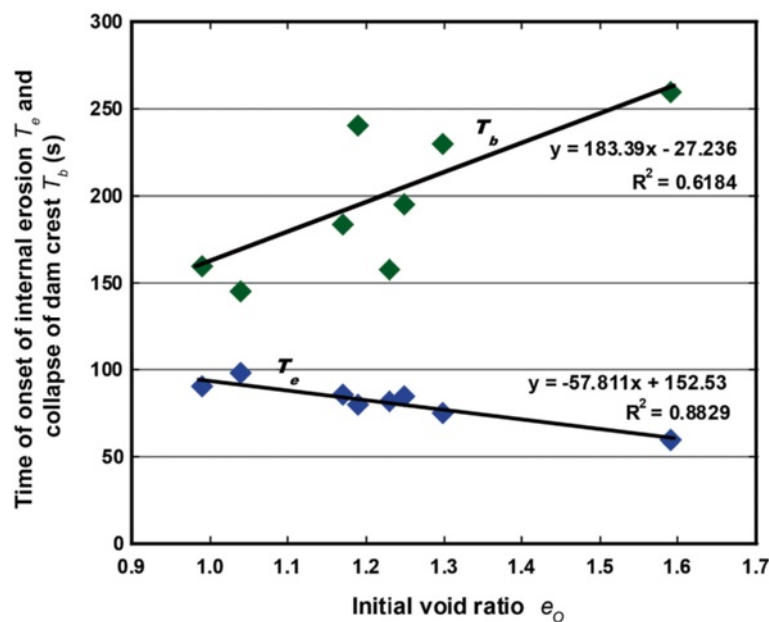
Fig. 13 Relationship between time of onset of internal erosion T_e, time of collapse of dam crest T_b and initial void ratio e_o
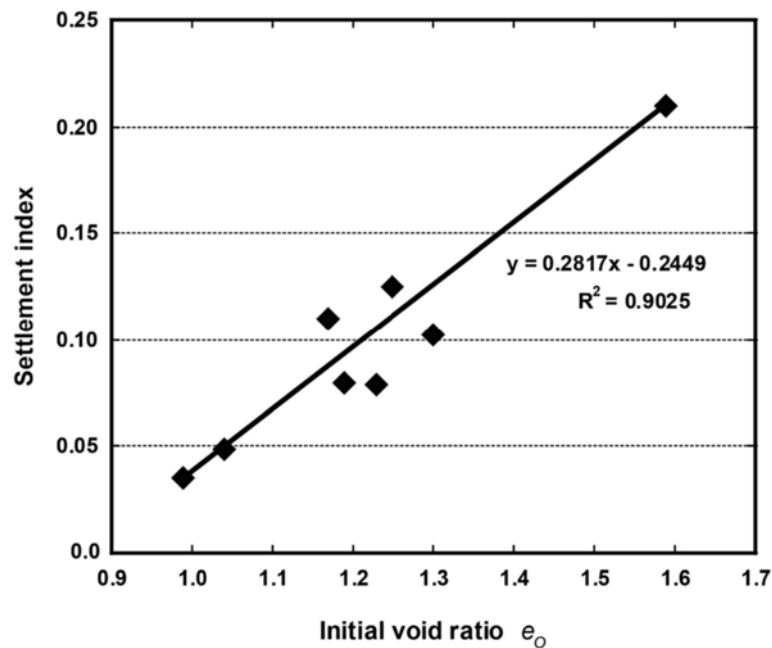
Fig. 14 Relationship between settlement index and initial void ratio e_o

in the initiation and development of piping in landslide dams, with emphasis on the potential failure mechanisms of dams composed of various soil materials. Landslide dams were built in a flume tank, and internal erosion within the dams was initiated using an artificial drainage channel composed of uniform pebbles encased in a plastic mesh. Initial condition assumed that the upstream lake was 'dry'. Thus, the upstream lake was recharged at a steady state flow rate of 1.2×10^{-4} m^3/s.

The various phases of the breach evolution process observed in this research included pipe development, pipe enlargement, crest settlement, hydraulic fracturing and unraveling of the downstream slope. The potential for formation of a continuous piping hole in dams composed of homogeneous soils decreased with an increase in bulk density and hydraulic conductivity. Dams composed of homogeneous soils failed mostly by seepage and downstream slope saturation (Dunning et al. 2006), whereas piping holes were formed in dams built with mixed soils, depending on the percentage fines content and the interlocking bonds between the soil particles.

This study did not measure erodibility coefficients of the dam materials, as it can be obtained from hole erosion tests (HET) (Wan and Fell 2004). However, it is evident from the results obtained here that the time of failure and the potential breach evolution mechanisms of the dams were controlled by soil density, including other factors such as void ratio, permeability and the degree of compaction, except in a few cases such as dam mix *D* (run series 4), where the interparticle bonds between the soil particles and low permeability of the

material affected soil erodibility. Early onset of internal erosion was observed in dams built with mixed materials, especially in the case of dam mix *A*. This condition may be attributed to suffusion, which caused adverse changes in permeability, porosity, void ratio and porewater pressure distribution in the soil. Conversely, the time of onset of internal erosion in the homogeneous dams increased with an increase in permeability.

Crest settlement and associated features such as cracking and hydraulic fracturing occurred in all the experiments, but were characteristically pronounced in the homogeneous dams, mostly in dams built with dam mixes *F* and *G*. The mechanism of dam crest collapse in dams built with mixed materials originated from two primary transverse cracks running parallel to the downstream slope, whereas the collapse mechanism of the homogeneous dams began from a longitudinal crack perpendicular to the downstream slope.

Although the breach evolution process observed in this study and the hydromechanical behaviour of the dams were constrained by space and time scales adapted in the flume experiments, the results provide valuable insights into the factors controlling the potential for seepage and piping failure of landslide dams. However, hole erosion tests (HET) need to be conducted on the finer materials used in these experiments to further evaluate the relationship between soil erodibility and hydraulic shear stress.

References
Awal, R., H. Nakagawa, M. Fujita, K. Kawaike, Y. Baba, and H. Zhang. 2011. Study on piping failure of natural dam. *Annuals of Disaster Prevention Research Institute Kyoto University* 54: 539–547.

Brauns, J. 1985. Stability of layered granular soil under horizontal groundwater flow. In *Proceedings of the 15th International Congress on Large Dams, vol 1, Lausanne*.

Capra, L. 2007. Volcanic natural dams: identification, stability, and secondary effects. *Natural Hazards* 43(1): 45–61.

Capra, L. 2011. Volcanic natural dams associated with sector collapses: textural and sedimentological constraints on their stability. In *Natural and Artificial Rockslide Dams*, ed. S.G. Evans, R.L. Hermanns, A. Strom, and G. Scarascia-Mugnozza, 279–294. Berlin Heidelberg: Springer.

Casagli, N., L. Ermini, and G. Rosati. 2003. Determining grain size distribution of material composing landslide dams in the Northern Apennines: sampling and processing methods. *Eng Geol (Amsterdam)* 69: 83–97.

Chang, D.S., L.M. Zhang, Y. Xu, and R.Q. Huang. 2011. Field testing of erodibility of two landslide dams triggered by the 12 May Wenchuan earthquake. *Landslides* 8(3): 321–332.

Charles, J.A. 1986. The significance of problems and remedial works at British earth dams. In *Proceedings of BNCOLD/IWES Conference on Reservoirs, Edinburgh*, 123–141.

Costa, J.E., and R.L. Schuster. 1988. The formation and failure of natural dams. *Geological Society of America Bulletin* 100: 1054–1068.

Crosta, G.B., P. Frattini, N. Fusi, and R. Sosio. 2006. Formation, characterization and modelling of the 1987 Val Pola rock-avalanche dam (Italy). *Italian J Eng Geol Envir, Special Issue* 1: 145–150.

Davies, T.R., and M.J. McSaveney. 2011. Rock-avalanche size and runout–implications for landslide dams. In *Natural and Artificial Rockslide Dams*, ed. S.G. Evans, R.L. Hermanns, A. Strom, and G. Scarascia-Mugnozza, 441–462. Berlin Heidelberg: Springer.

Duman, T.Y. 2009. The largest landslide dam in Turkey: Tortum landslide. *Engineering Geology* 104(1): 66–79.

Dunning, S.A. 2006. The grain-size distribution of rock avalanche deposits in valley-confined settings. *Italian J Eng Geol Environ* 1: 117–121.

Dunning, S.A., and P.J. Armitage. 2011. The grain-size distribution of rock-avalanche deposits: implications for natural dam stability. In *Natural and Artificial Rockslide Dams*, ed. S.G. Evans, R.L. Hermanns, A. Strom, and G. Scarascia-Mugnozza, 479–498. Berlin Heidelberg: Springer.

Dunning, S.A., N.J. Rosser, D.N. Petley, and C.R. Massey. 2006. Formation and failure of the Tsatichhu landslide dam, Bhutan. *Landslides* 3(2): 107–113.

Faulkner, H. 2006. Piping hazard on collapsible and dispersive soils in Europe. *Soil Erosion in Europe* 537–562

Fell, R., C.F. Wan, J. Cyganiewicz, and M. Foster. 2003. Time for development of internal erosion and piping in embankment dams. *Journal of Geotechnical and Geoenvironmental Engineering* 129(4): 307–314.

Fox, G.A., R.G. Felice, T.L. Midgley, G.V. Wilson, and A.S. Al-Madhhachi. 2014. Laboratory soil piping and internal erosion experiments: evaluation of a soil piping model for low-compacted soils. *Earth Surface Processes and Landforms* 39(9): 1137–1145.

Fread, D.L. 1988. *The NWS DAMBRK model: Theoretical background/user documentation*. National Weather Service, NOAA: Hydrologic Research Laboratory.

Glazyrin, G.Y., and V.N. Reyzvikh. 1968. Computation of the flow hydrograph for the breach of landslide lakes. *Soviet Hydrology* 5: 492–496.

Hanson, G.J., and K.R. Cook. 1997. *Development of excess shear stress parameters for circular jet testing*, vol. ASAE Paper No. 972227. St Joseph: American Society of Agricultural Engineering.

Hanson, G.J., and K.M. Robinson. 1993. The influence of soil moisture and compaction on spillway erosion. *Transactions of the ASAE* 36(5): 1349–1352.

Hanson, G.J., R.D. Tejral, S.L. Hunt, and D.M. Temple. 2010. Internal erosion and impact of erosion resistance. In *Proceedings of the 30th US Society on Dams Annual Meeting and Conference, Sacramento, California*, 773–784.

Jones, J.A.A. 1994. Soil piping and its hydrogeomorphic function. *Cuaternario y Geomorfologia* 8(3–4): 77–102.

Jones, J.A.A. 2004. Implications of natural soil piping for basin management in upland Britain. *Land Degradation & Development* 15(3): 325–349.

Ke, L., and A. Takahashi. 2012. Influence of internal erosion on deformation and strength of gap-graded non-cohesive soil. In *Proceedings of the Sixth International Conference on Scour and Erosion, Paris*, 847–854.

Korup, O. 2004. Geomorphometric characteristics of New Zealand landslide dams. *Engineering Geology* 73(1): 13–35.

Maknoon, M., and T.F. Mahdi. 2010. Experimental investigation into embankment external suffusion. *Natural Hazards* 54(3): 749–763.

Marot, D., F. Bendahmane, and H.H. Nguyen. 2012. Influence of angularity of coarse fraction grains on internal erosion process. In *Proceedings of the Sixth International Conference on Scour and Erosion, Paris*, 887–894.

Masannat, Y.M. 1980. Development of piping erosion conditions in the Benson area, Arizona, USA. *Quarterly Journal of Engineering Geology and Hydrogeology* 13(1): 53–61.

Mattsson, H., J.G.I. Hellström, and T.S. Lundström. 2008. *On internal erosion in embankment dams*. Research Report: Luleå University of Technology. Retrieved from http://epubl.ltu.se/1402-1528/2008/14/LTU-FR-0814-SE.pdf.

Mora, S., C. Madrigal, J. Estrada, and R.L. Schuster. 1993. The 1992 Rio Toro landslide dam, Costa Rica. *Landslide News* 7: 19–22.

Okeke, A.C., F. Wang, T. Sonoyama, and Y. Mitani. 2013. Laboratory experiments on landslide dam failure due to piping: An evaluation of 2011 typhoon-induced landslide and landslide dam in Western Japan. In *Progress of Geo-Disaster Mitigation Technology in Asia*, ed. F.W. Wang, M. Miyajima, T. Li, S. Wei, and T.F. Fathani, 525–545. Berlin Heidelberg: Springer.

Pushkarenko, V.P., and A.M. Nikitin. 1988. Experience in the regional investigation of the state of mountain lake dams in Central Asia and the character of breach mudflow formation. In *Landslides and Mudflows*, ed. E. Kozlovskii, 359–362. Moscow: UNEP/UNESCO.

Richards, K.S., and K.R. Reddy. 2012. Experimental investigation of initiation of backward erosion piping in soils. *Geotechnique* 62(10): 933–942.

Schuster, R.L. 1995. Landslide dams-a worldwide phenomenon. In *Proceedings of the Annual Symposium of the Japanese Landslide Society, Kansai Branch, Osaka*, 1–23.

Shugar, D.H., and J.J. Clague. 2011. The sedimentology and geomorphology of rock avalanche deposits on glaciers. *Sedimentology* 58(7): 1762–1783.

Sidle, R.C., H. Kitahara, T. Terajima, and Y. Nakai. 1995. Experimental studies on the effects of pipeflow on throughflow partitioning. *Journal of Hydrology* 165(1): 207–219.

Singh, V. 1996. *Dam breach modeling technology*. Water Science and Technology Library: Kleiwer Academic Publishers.

Stene, E.A. 1995. *The Teton Basin Project: (Second Draft)*.. Bureau of Reclamation History Program.

Strom, A. 2013. Geological prerequisites for landslide dams' disaster assessment and mitigation in Central Asia. In *Progress of Geo-Disaster Mitigation Technology in Asia*, ed. F.W. Wang, M. Miyajima, T. Li, S. Wei, and T.F. Fathani, 17–53. Berlin Heidelberg: Springer.

Wan, C.F., and R. Fell. 2004. Investigation of rate of erosion of soils in embankment dams. *Journal of Geotechnical and Geoenvironmental Engineering* 130(4): 373–380.

Wang, G., R. Huang, T. Kamai, and F. Zhang. 2013. The internal structure of a rockslide dam induced by the 2008 Wenchuan (M_w 7.9) earthquake, China. *Engineering Geology* 156: 28–36.

Wassmer, P., J.L. Schneider, N. Pollet, and C. Schmitter-Voirin. 2004. Effects of the internal structure of a rock–avalanche dam on the drainage mechanism of

its impoundment, Flims sturzstrom and Ilanz paleo-lake, Swiss Alps. *Geomorphology* 61(1): 3–17.

Weidinger, J.T. 2006. Landslide dams in the high mountains of India, Nepal and China-stability and life span of their dammed lakes. *Italian Journal of Engineering Geology and Environment* 1: 67–80.

Wilson, G.V. 2009. Mechanisms of ephemeral gully erosion caused by constant flow through a continuous soil-pipe. *Earth Surface Processes and Landforms* 34(14): 1858–1866.

Wilson, G. 2011. Understanding soil-pipe flow and its role in ephemeral gully erosion. *Hydrological Processes* 25(15): 2354–2364.

Wit, J.D., J.B. Sellmeijer, and A. Penning. 1981. *Laboratory testing on piping*, 517–520. In: Tenth International Conference on Soil Mechanics and Foundation Engineering.